



## RESEARCH ARTICLE

# Photobiomodulation therapy at 632 nm wavelength ameliorates intrauterine adhesion via activation of cAMP/PKA/CREB pathway

Hongjie Zheng<sup>1</sup> | Caixia Wang<sup>1,2</sup> | Shan Wu<sup>1</sup> | Qing Pei<sup>1</sup> | Min Yao<sup>1</sup> 

<sup>1</sup>Department of Plastic and Reconstructive Surgery, Shanghai Ninth People's Hospital, Shanghai Jiao Tong University, School of Medicine, Shanghai, China

<sup>2</sup>Shanghai Institute of Laser Technology, Shanghai, China

## Correspondence

Min Yao, Department of Plastic and Reconstructive Surgery, Shanghai Ninth People's Hospital, Shanghai Jiao Tong University, School of Medicine, Shanghai 200011, China.  
Email: [my058@vip.sina.com](mailto:my058@vip.sina.com)

## Funding information

National Key Research Program of China, Grant/Award Number: 2018YFC1004803 and 2020YFC1512704; Science and Technology Commission of Shanghai Municipality, Grant/Award Number: 22MC1940300

## Abstract

Intrauterine adhesion (IUA), a major cause of uterine infertility, is pathologically characterized by endometrial fibrosis. Current treatments for IUA have poor efficacy with high recurrence rate, and restoring uterine functions is difficult. We aimed to determine the therapeutic efficacy of photobiomodulation (PBM) therapy on IUA and elucidate its underlying mechanisms. A rat IUA model was established via mechanical injury, and PBM was applied intrauterinely. The uterine structure and function were evaluated using ultrasonography, histology, and fertility tests. PBM therapy induced a thicker, more intact, and less fibrotic endometrium. PBM also partly recovered endometrial receptivity and fertility in IUA rats. A cellular fibrosis model was then established with human endometrial stromal cells (ESCs) cultured in the presence of TGF- $\beta$ 1. PBM alleviated TGF- $\beta$ 1-induced fibrosis and triggered cAMP/PKA/CREB signaling in ESCs. Pretreatment with the inhibitors targeting this pathway weakened PBM's protective efficacy in the IUA rats and ESCs. Therefore, we conclude that PBM improved endometrial fibrosis and fertility via activating cAMP/PKA/CREB signaling in IUA uterus. This study sheds more lights on the efficacy of PBM as a potential treatment for IUA.

## KEYWORDS

632 nm laser, fibrosis, intrauterine adhesion, photobiomodulation, reproductive

## INTRODUCTION

Intrauterine adhesion (IUA), or Asherman's syndrome, has the pathological characterization of a completely or partially blocked uterine cavity caused by endometrial

fibrosis, mainly resulting from endometrial injury or infection.<sup>1</sup> IUA is the most common cause of secondary infertility in females and can lead to other problems in the reproductive system, such as hypomenorrhea, amenorrhea, and recurrent abortion.<sup>1</sup> Therefore, uterine cavity

**Abbreviations:** AC, adenyl cyclase; ANOVA, one-way analysis of variance; ART, assisted reproductive technology; BSA, bovine serum albumin; cAMP, cyclic adenosine monophosphate; CCO, cytochrome C oxidase; COL1, collagen type 1; CREB, cAMP-responsive element binding protein; E, embryonic day; ECM, extracellular matrix; EECs, endometrial epithelial cells; ELISA, enzyme-linked immunosorbent assay; ESCs, endometrial stromal cells; FN1, fibronectin 1; HE, hematoxylin-eosin; IHC, immunohistochemistry; IUA, intrauterine adhesion; NO, nitric oxide; PBM, photobiomodulation; PKA, cAMP-dependent protein kinase; RT, room temperature; TGF- $\beta$ 1, transforming growth factor- $\beta$ 1;  $\alpha$ -SMA,  $\alpha$ -smooth muscle actin.

Hongjie Zheng and Caixia Wang contributed equally to this study.

reconstruction and uterine function restoration are prioritized when treating IUA. To date, the most widely used intervention for IUA is hysteroscopic adhesiolysis combined with various adjuvant therapies.<sup>1,2</sup> Although these treatments can temporarily restore the morphology of the uterus to varying degrees, the poor efficacy and high recurrence rate of IUA persist.<sup>3</sup> Hence, efficient complementary interventions for IUA are urgently required.

Photobiomodulation (PBM) therapy uses near-infrared or red lasers at non-thermal irradiance (output power lower than 500 mW) to regulate biological activity without heating the tissue.<sup>4</sup> PBM has been widely used to facilitate wound healing, alleviate inflammation, and reduce pain.<sup>5–7</sup> The potential anti-fibrotic effects of PBM at various wavelengths on diverse cells and tissues have been reported.<sup>8,9</sup> Furthermore, the few studies focusing on female reproductive diseases have suggested that PBM increased endometrial cell proliferation and the expression of endometrial receptivity genes *in vitro*.<sup>10,11</sup> Thus, PBM seems to have great potential for reducing fibrosis and promoting endometrial regeneration. However, whether PBM attenuates endometrial fibrosis and impaired fertility caused by IUA remains unclear.

In the present study, we established a rat IUA model and evaluated the therapeutic efficacy of PBM at 632 nm on uterine morphology and function. Moreover, we investigated the underlying mechanisms by utilizing a cellular fibrosis model established by culturing endometrial stromal cells (ESCs) in the presence of TGF- $\beta$ 1 with a specific focus on the signaling cascades stimulated by PBM.

## MATERIALS AND METHODS

### Animals and IUA model

Forty-five 7-week-old Sprague–Dawley rats (40 female, 5 male) were provided by Shanghai Laboratory Animal Center, Chinese Academy of Sciences. All experiments were approved by the Animal Care and Experiment Committee of Shanghai Jiao Tong University School of Medicine (approval number: SH9H-2020-A741-1).

After acclimatization for a week, the rats were subjected to mechanical injury for IUA model establishment, as described by a previous study.<sup>12</sup> Briefly, 30 female rats were subjected to anesthesia via intraperitoneal injection with 3% sodium pentobarbital (1 mL/kg). Afterwards, the midline of the abdomen was incised longitudinally for 5 cm using ophthalmic scissors. The right uterus was exposed, and an incision of 2 mm was generated in the uterus 5 mm close to the ovary. A 16-gauge needle was inserted into the uterus, passed through this incision, and scratched the

endometrium to make the wall of uterus pale and rough (5–7 passes/direction, 3 directions). The left uterus was not scratched as a control group. Nine days (two estrous cycles) after uterus damage, the animals were randomized into two groups (15 rats per group). For the IUA + PBM group, PBM treatment was applied on the right uterus of the rats, while the rats in the IUA group were not treated. For histological analysis, uterine tissues were obtained from 10 sacrificed rats 9 days after treatment. The remaining 20 rats were used in the mating test. **Figure 1A** illustrates the study design.

For the mechanism elucidation experiment, IUA was established on the bilateral uteri of 10 rats. The IUA rats were then intraperitoneally injected with PBS or SQ22536 (10  $\mu$ g/day,  $n = 5$ ) for continuous 7 days. The right uteri were treated with PBM, and 9 days later, mating test was performed.

### PBM therapy

A 40-mW laser device generating 632-nm lights (MY-LA001; Shanghai Well Medical Technology Co., Ltd) was utilized for PBM (**Table 1**). The irradiance was measured at the target surface by a power meter (Ophir). A laser fiber with a diameter of 1.7 mm and a length of 2 cm was used for the *in vivo* study. For emission, the fiber was placed inside the uterine cavity of rats for 10 min (**Figure 1B**). An energy fluence of 5.29 J/cm<sup>2</sup> in the continuous mode was applied to the uterus in the IUA + PBM group. The uteri of the IUA group underwent the same surgical procedure but without laser irradiation. For the cell experiments, we customized the spot size of the laser to make sure that the entire surface area of the 3.5-cm culture dish was exposed to the laser with a dose of 1.5 J/cm<sup>2</sup>.

### Mating test

Nine days after the treatment, a mating test was performed between the female IUA and healthy male rats under a ratio of 2:1 for 4 days. After another 14 days, the female rats were sacrificed, and the number of embryos was recorded.

For endometrial receptivity analysis, the IUA rats were mated with male rats overnight. The morning when sperms were seen on vaginal smear was considered embryonic day 0.5 (E 0.5). At E 4.5, the implantation sites were visualized through intravenous injection of Trypan Blue solution (MedChemExpress).<sup>13</sup> The uteri were then collected for histological analysis.

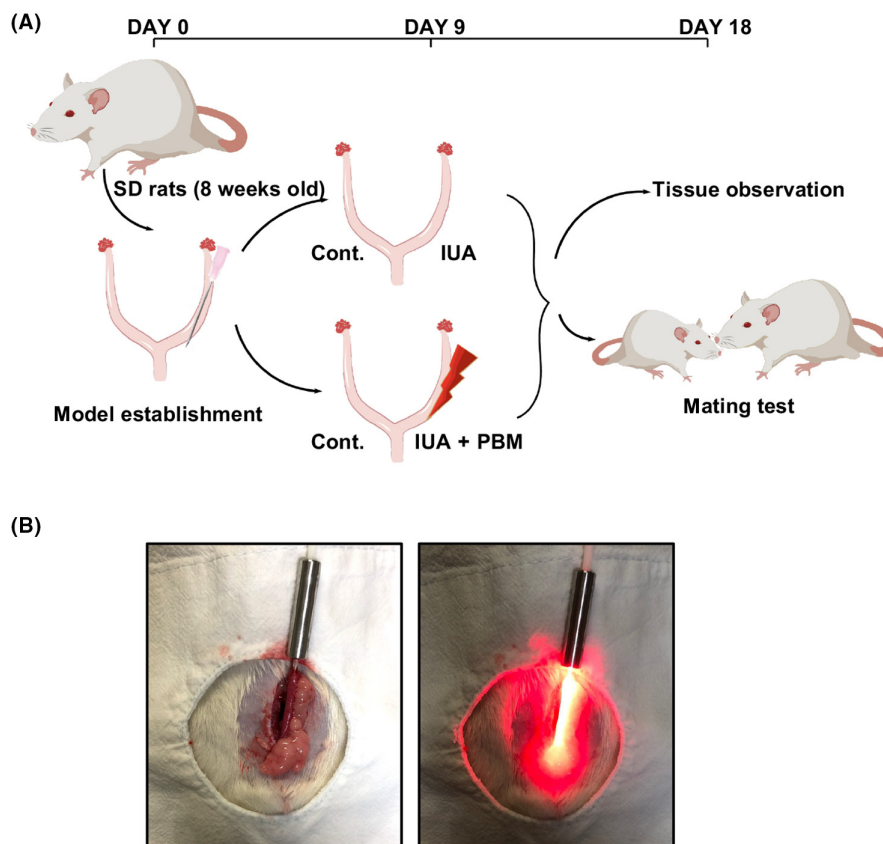


**FIGURE 1** Schema of photobiomodulation (PBM) therapy as an intrauterine intervention for the treatment of intrauterine adhesion (IUA). (A) The design of the in vivo study. (B) Insertion of the fiber into the uterus and laser emission.

**TABLE 1** Irradiance parameters for photobiomodulation therapy.

	In vivo	In vitro
Wavelength (nm)	632	632
Operating mode	CW	CW
Output power (mW)	40	40
Sessions	1	1
Distance to tissue/cells (cm)	0.1	8
Spot size at target (cm <sup>2</sup> )	4.54	8
Irradiance (mW/cm <sup>2</sup> )	8.81	4.99
Exposure duration (min)	10	5
Energy density (J/cm <sup>2</sup> )	5.29	1.50
Total radiant energy (J)	24	12

Abbreviation: CW, continuous wave.

## Ultrasound examination

Rats were anesthetized and placed in the prone position after preparation of the dorsal skin 9 days after treatment. Ultrasound examination (Philips) was conducted by a trained sonographer to evaluate uterine health.

## Histological staining

Uteri were subjected to fixation, dehydration and paraffin embedding. Afterwards, 5- $\mu$ m-thick sections were prepared and stained with hematoxylin-eosin (HE) and Masson for morphological assessment. Endometrial thickness was calculated as the ratio of endometrial area to the circumference at the junction of endometrium and myometrium.<sup>14</sup> For Masson staining, the percentage of blue-stained areas of collagen fibers was measured. For immunohistochemistry (IHC) staining, the slides were incubated with anti-collagen1, anti-CK18, or anti-Ki67 antibodies (Abcam), and then with horseradish peroxidase-labeled secondary antibodies (Beyotime). The intensity of staining was classified as 0 (negative), 1 (weak), 2 (intermediate), or 3 (strong).<sup>15</sup> The slides were finally photographed with a light microscope (Nikon). All quantitative measurements were performed using ImageJ (National Institutes of Health).

## Culturing and treatment of cells

Human ESCs were purchased from ATCC (KC02-44D, ATCC SC-6000). DMEM containing 10% fetal bovine

serum, 10 mM HEPES, 100 U/mL penicillin, 100 µg/mL streptomycin, and 2 µg/mL blasticidine was used to maintain the growth of ESCs at 37°C. The cells were passaged at 80%–90% confluence.

To induce fibrosis, cells were cultured for 24 h in the presence of TGF-β1 at concentrations of 0, 5, 10, or 20 ng/mL. Afterwards, mRNA and protein levels of FN1, COL1, and α-SMA were measured. To explore the effect of PBM on cellular fibrosis, the ESCs were plated in 3.5-cm dishes and irradiated after the treatment of TGF-β1, as described by previous studies.<sup>8,16</sup> Twenty-four hours later, total mRNA and protein were extracted for further evaluation. To explore whether the cAMP signaling pathway is involved in the response to PBM, the cells were incubated with adenylyl cyclase inhibitor SQ22536 (10 µM), PKA inhibitor H-89 (10 µM), or CREB inhibitor KG501 (25 µM) (MedChemExpress) for 1 h before TGF-β1 and PBM treatment.

## RNA extraction and quantitative PCR

Total RNA was extracted using a extraction reagent (EZBioscience), and the concentration was measured using a NanoDrop spectrophotometer (ThermoScientific). Another kit from EZBioscience was utilized for reverse transcription of the isolated total RNA and qPCR was carried out with a qPCR kit from the same vendor based on the fluorescence dye SYBR Green. The following primers were synthesized by Shanghai Sangon Biotech: GAPDH sense 5'-CTCCTCTGACTTCAACAGCG-3' and anti-sense 5'-TTCGTTGTCATACCAGGAAATGAG-3'; FN1 sense 5'-ATTCATGGGAGAAGTATGTGCATG-3' and anti-sense 5'-AGGACCACTTGAGCTTGGATAG-3'; COL1A1 sense 5'-AGCCAGCAGATCGAGAACAT-3' and anti-sense 5'-GGTCAATCCAGTACTCTCCACT-3'. α-SMA sense 5'-TCAGGGGGCACCCTATGT-3' and anti-sense 5'-CGGAGGGGCAATGATCTTGAT-3'; PKA sense 5'-AC CTCCTGCAGGTAGATCTCA-3' and anti-sense 5'-AT GAAGGGAGCTTCCACCTTC-3'; CREB sense 5'-CAAGG AGGCCTTCCTACAGG-3' and anti-sense 5'-CCGTTACA GTGGTGATGGCA-3'.

## Western blotting

Whole cell lysates of ESCs were prepared with RIPA lysis buffer added with inhibitors against phosphatase and protease (Beyotime), and determined for protein concentration via the BCA method. SDS-PAGE was then implemented to separate the proteins, which were then electrotransferred onto PVDF membranes (Millipore). The membranes were incubated at room temperature

(RT) in 5% non-fat milk, washed, and subjected to overnight incubation in primary antibodies. Then the membranes were washed and subjected to incubation in secondary antibodies labeled with horseradish peroxidase for 60 min. Protein bands were visualized using chemiluminescence kits (ThermoScientific) by the BioImaging System (Bio-Rad).

## Immunofluorescence and phalloidin staining

Endometrial stromal cells were incubated for 15 min in 4% paraformaldehyde, washed thrice (5 min each) by 0.01% Triton X-100, immersed for 1 h in 1% bovine serum albumin (BSA), and subjected to overnight incubation at 4°C in a diluted anti-α-SMA antibody (Cell Signaling Technology). Then the cells were rinsed and labeled by fluorescein (FITC)-conjugated secondary antibodies and phalloidin conjugated with Alexa Fluor 594 (Beyotime) at RT for 40 min. DAPI (ThermoScientific) was used to visualize the nucleus. Cells were photographed under a Carl Zeiss confocal microscope.

## Cellular cAMP content measurement

Cellular cAMP content was detected by enzyme-linked immunosorbent assay (ELISA). The cells were collected, lysed, and the lysate was centrifuged to remove debris. The supernatant was processed according to the manufacturer's instructions (GenScript) and analyzed using an Infinite M200pro spectrophotometer (Tecan).

## Statistical analysis

The statistical results are displayed as mean ± standard deviation (SD). One-way analysis of variance (ANOVA) with post-hoc tests was performed in SPSS software (IBM) to analyze differences among groups, with  $p < 0.05$  representing statistical significance. All graphs were processed with GraphPad Prism (GraphPad Software) or Adobe Illustrator CC software (Adobe).

## RESULTS

### PBM improves uterine morphology in IUA rats

A rat IUA model was established through mechanical injury and treated with or without PBM to explore the effect of PBM on uterine morphology. Two-dimensional

ultrasound exhibited continuous, uniform endometrial line centered in the uterine cavity for rats in the control group (Figure 2A). The echo of endometrium was undetectable in most areas of the uterus for rats in the

IUA group, and the visible part was obscure and not in the middle of the cavity. After PBM treatment, the echogenic signal of the endometrium partially recovered, with improved intensity and continuity. In addition, gross

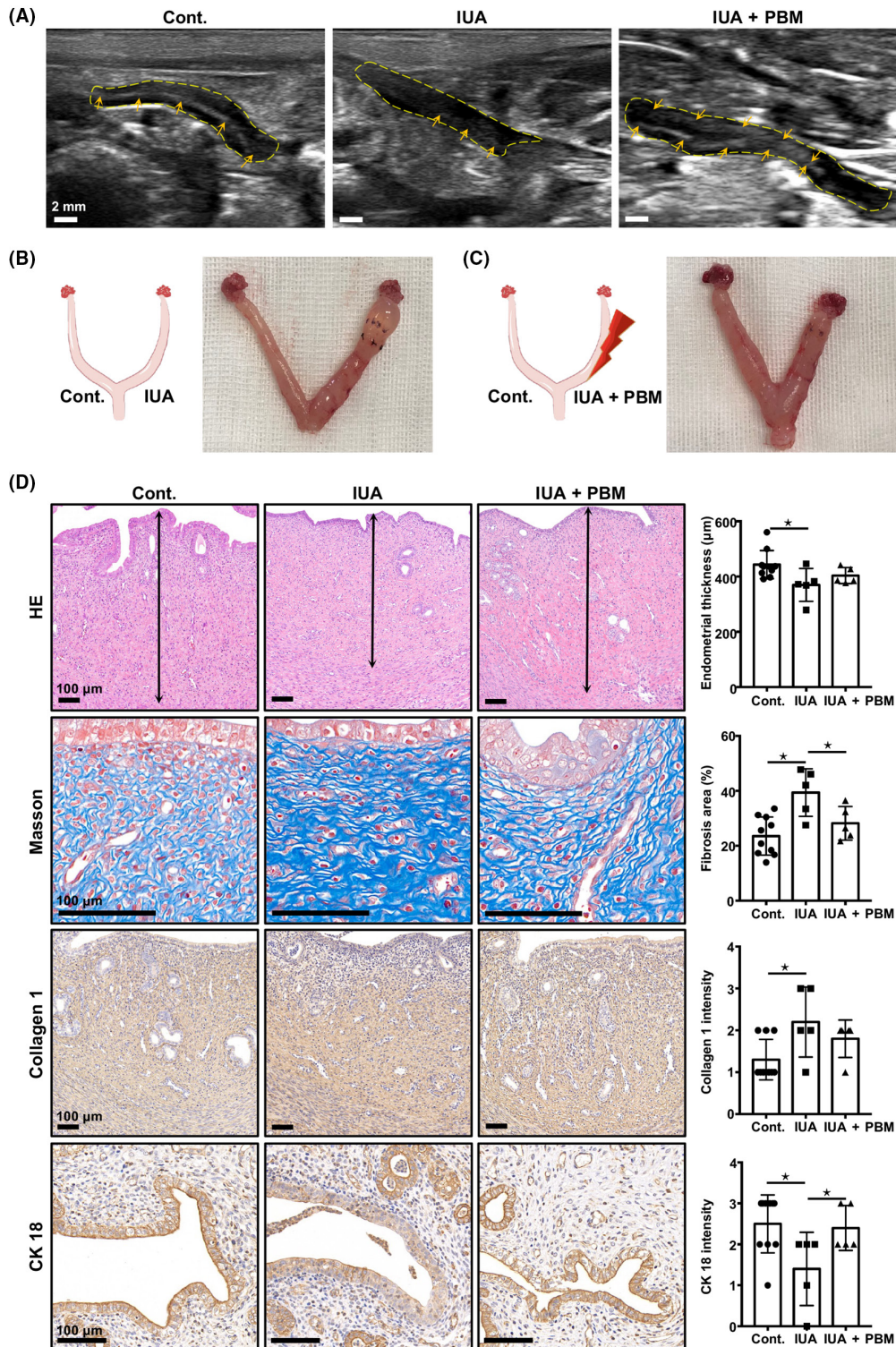


**FIGURE 2** Photobiomodulation (PBM) ameliorates uterine morphology in intrauterine adhesion (IUA) rats. (A) Ultrasound examination of the uterus at 9 days after treatment. Dotted lines indicate the uterine cavity. Arrows indicate the endometrial line. Scale bars = 2 mm. (B, C) Gross images of uteri at 9 days after treatment. (D) Histological staining of uteri at 9 days after treatment. Scale bars = 100  $\mu\text{m}$ . \* $p < 0.05$ .

observation revealed that the IUA uterus had obvious uterine edema with hydrometra and slight stenosis compared to the control group (Figure 2B). With PBM treatment, the general condition of the IUA uterus was partially restored, with mild hyperemia and no obvious stenosis or atrophy (Figure 2C). Furthermore, we evaluated the microstructure of the IUA uterus using histological analysis 9 days after treatment (Figure 2D). HE sections of endometrium in the control group had a single columnar epithelium layer and dispersed glands in the basal layer and submucosa, revealing normal endometrium morphology. The endometrium of IUA rats was significantly thinner compared with that of control rats ( $370 \pm 60$  vs.  $443 \pm 51 \mu\text{m}$ ;  $p < 0.05$ ). This reduction was partially restored by PBM ( $403 \pm 29 \mu\text{m}$ ;  $p > 0.05$ ), indicating the endometrium-regenerating effect of PBM. To evaluate endometrial fibrosis, Masson staining and IHC for collagen 1 were performed. Collagen deposition was more evident in the IUA group ( $39 \pm 9\%$ ) than in control ( $24 \pm 7\%$ ) and IUA+ PBM groups ( $28 \pm 6\%$ ) ( $p < 0.05$ ). Regarding the regeneration of endometrial epithelial cells (EECs), further IHC for CK18 demonstrated that significantly less CK18-positive EECs were found in the IUA group compared to the other two groups ( $p < 0.05$ ). Collectively, the findings indicate that PBM improves the morphological recovery of the uterus after uterine injury in vivo.

### PBM enhances fertility and endometrial receptivity in IUA rats

We then determined whether the injured uterus of IUA rats could accept embryos and support embryo development into late gestation after PBM treatment. The rats were mated, and embryos within the pregnant uteri were harvested on gestational day 15–18 (Figure 3A,B). All uteri in the control group were pregnant (100%), and IUA uteri treated with PBM exhibited a much higher pregnancy rate (60%) than those without PBM treatment (20%). Meanwhile, the IUA uteri had significantly fewer embryos ( $p < 0.05$ ), implying that PBM partially recovered the reproductive ability of IUA rat uterus.

Endometrial receptivity, which refers to a transient endometrium maturation period in which the endometrium can accept blastocyst attachment and implantation,<sup>17</sup> was further evaluated. It is generally recognized that IUA causes impaired endometrial receptivity, leading to implantation failure and poor pregnancy outcomes.<sup>18</sup> As shown in Figure 3C, the IUA uterus had fewer implantation sites at E 4.5 than the other groups. Ki67 expression in the endometrium was also analyzed at E 4.5, as non-proliferative epithelium at E 4.5 is a hallmark of endometrial receptivity.<sup>19</sup> The increase in the number of

Ki67-positive EECs by IUA was obviously reduced after PBM ( $p < 0.05$ ) (Figure 3D,E). These data verify that PBM facilitated the recovery of fertility function of the injured uterus in vivo.

### PBM alleviates TGF- $\beta$ 1-induced ESCs fibrosis in vitro

To verify our in vivo results, human ESCs were treated with TGF- $\beta$ 1 to mimic cellular fibrosis in the IUA animal model. TGF- $\beta$ 1 activated ESCs into myofibroblasts and induced the expressions of cytoskeleton and extracellular matrix (ECM) in ESCs with no significant differences between concentrations (see Figure S1). Finally, 5 ng/mL of TGF- $\beta$ 1 was selected to induce fibrosis in ESCs in subsequent experiments.

To determine whether PBM improves TGF- $\beta$ 1-induced ESCs fibrosis, ESCs were treated with TGF- $\beta$ 1 and immediately received PBM. The increased mRNA and protein levels of ECM after TGF- $\beta$ 1 treatment were markedly reduced by PBM (Figure 4A,B). We further evaluated the expressions of  $\alpha$ -SMA and F-actin via immunofluorescence and phalloidin staining. After treatment with PBM, the increased fluorescence intensity of  $\alpha$ -SMA in TGF- $\beta$ 1-treated ESCs was reduced (Figure 4C). These results demonstrate that PBM alleviates TGF- $\beta$ 1-induced ESCs fibrosis in vitro.

### PBM attenuates fibrosis through cAMP/PKA/CREB signaling pathway

It has been reported that PBM irradiation increases cellular cAMP levels.<sup>20,21</sup> To determine whether the cAMP signaling contributed to the fibrosis-preventing effect of PBM, we first measured cAMP contents in ESCs using ELISA (Figure 5A). TGF- $\beta$ 1 treatment decreased cAMP contents, which were reversed by PBM irradiation ( $p < 0.05$ ). In addition, PBM increased the transcription of PKA and CREB genes and promoted the phosphorylation of these two proteins, which are downstream molecules of cAMP (Figure 5B,C). These data reveal that PBM activates cAMP/PKA/CREB signaling pathway.

We next assessed the effects of PBM on cells pretreated with inhibitors of cAMP/PKA/CREB signaling. After incubation with SQ22536 (an adenylyl cyclase inhibitor), H-89 (a PKA inhibitor), or KG501 (a CREB inhibitor), the levels of phosphorylated PKA and CREB declined significantly (Figure 5D,F,H). Most importantly, the effect of PBM on reducing ECM expression in TGF- $\beta$ 1-treated ESCs was significantly decreased after treatment with cAMP signaling inhibitors (Figure 5E,G,I). To validate these results in vivo, IUA rats

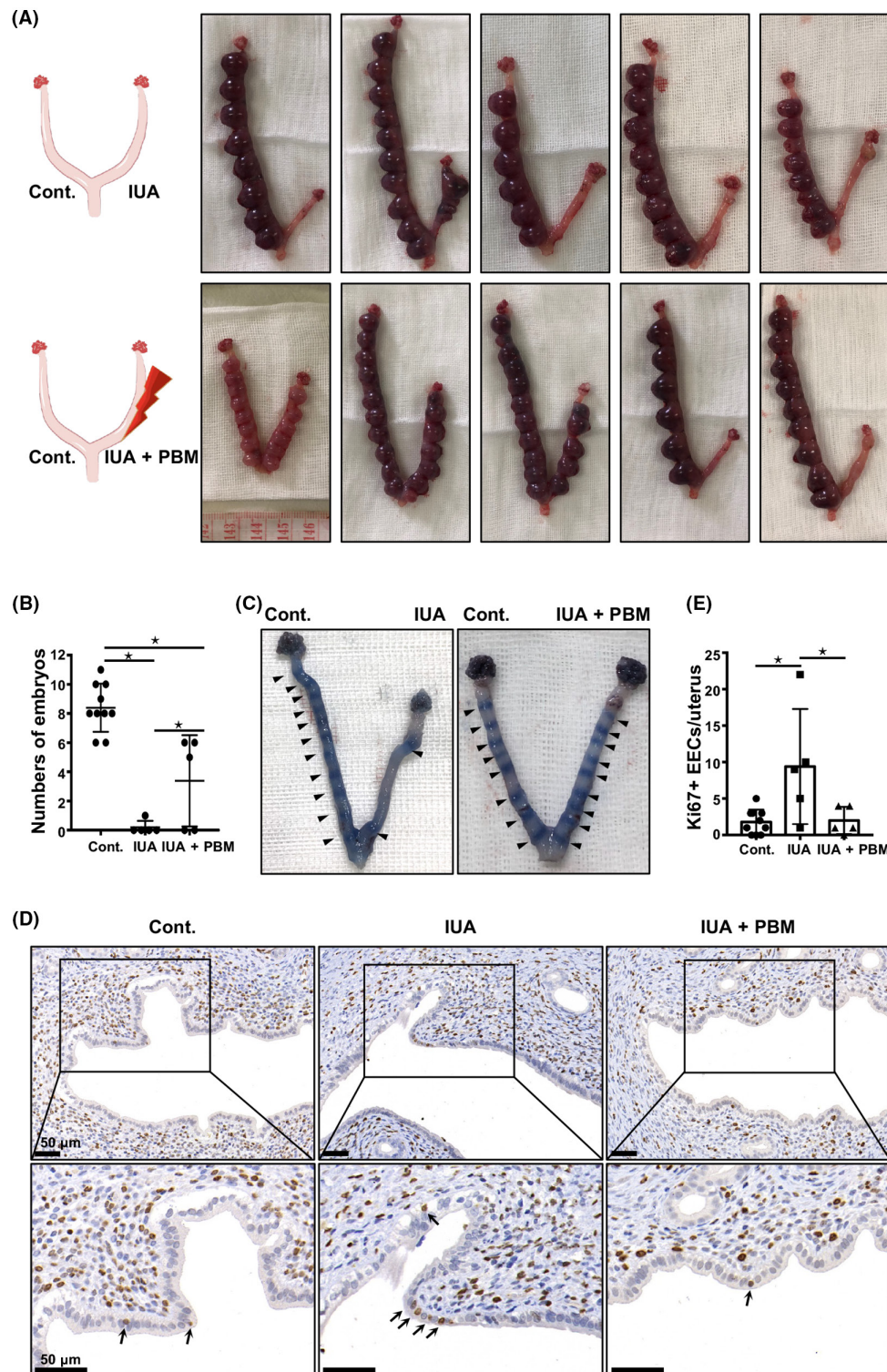


**FIGURE 3** Photobiomodulation (PBM) enhances fertility and endometrial receptivity in intrauterine adhesion (IUA) rats. (A) Pregnant outcomes of IUA rats at gestational day 15–18. (B) Numbers of embryos at gestational day 15–18. \* $p < 0.05$ . (C) Trypan Blue dye staining of the uteri at embryonic day 4.5. Arrows indicate the implantation sites. (D) Immunohistochemistry for Ki67 at embryonic day 4.5. Arrows indicate Ki67-positive endometrial epithelial cells (EECs). Scale bars = 50 μm. (E) Numbers of Ki67-positive EECs per uterus at embryonic day 4.5. \* $p < 0.05$ .

were intraperitoneally injected with SQ22536 (10 μg/day) before PBM. Pregnancy outcomes analysis showed that PBM increased the number of embryos reduced by IUA. However, treatment with the cAMP inhibitor

eliminated the protective effect of PBM (Figure 5J). Taken together, our findings demonstrate the crucial role of cAMP/PKA/CREB signaling in the effect of PBM on IUA in vitro and in vivo.

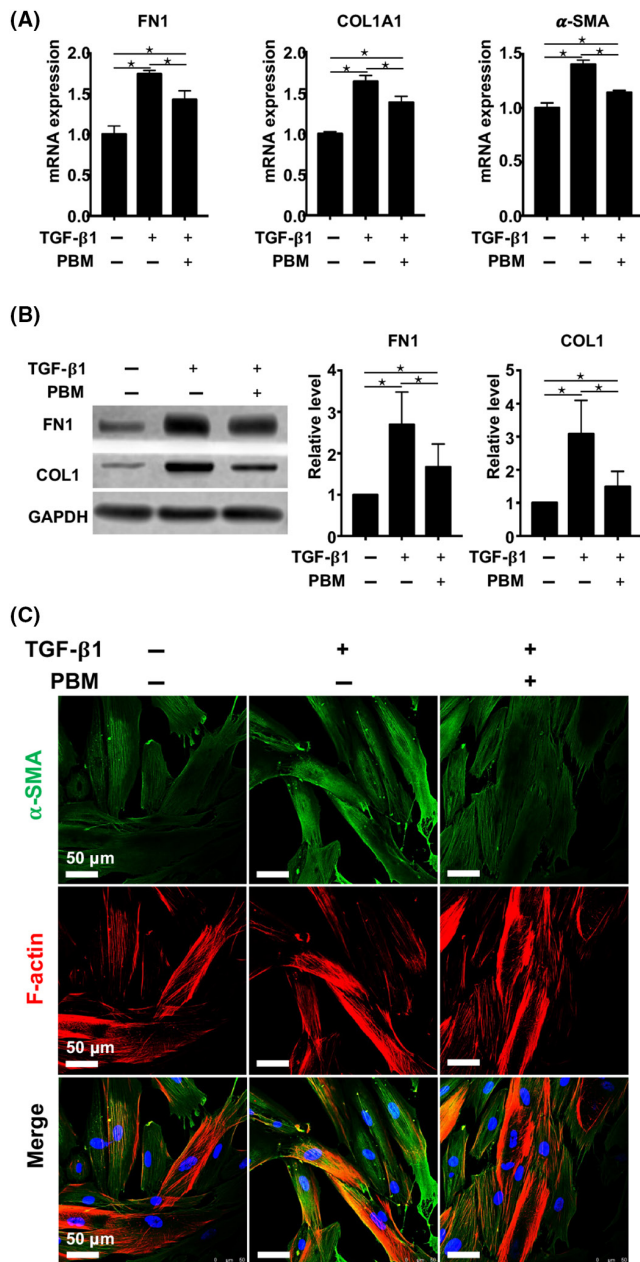


**FIGURE 4** Photobiomodulation (PBM) alleviates TGF- $\beta$ 1-induced endometrial stromal cells (ESCs) fibrosis in vitro. (A) The mRNA expressions of FN1, COL1A1, and  $\alpha$ -SMA in ESCs after treatment with TGF- $\beta$ 1 and PBM for 24 h.  $*p < 0.05$ . (B) The protein expressions of FN1 and COL1 in ESCs after treatment with TGF- $\beta$ 1 and PBM for 24 h.  $*p < 0.05$ . (C) The  $\alpha$ -SMA and F-actin staining of ESCs after treatment with TGF- $\beta$ 1 and PBM for 24 h. Scale bars = 50  $\mu$ m.

## DISCUSSION

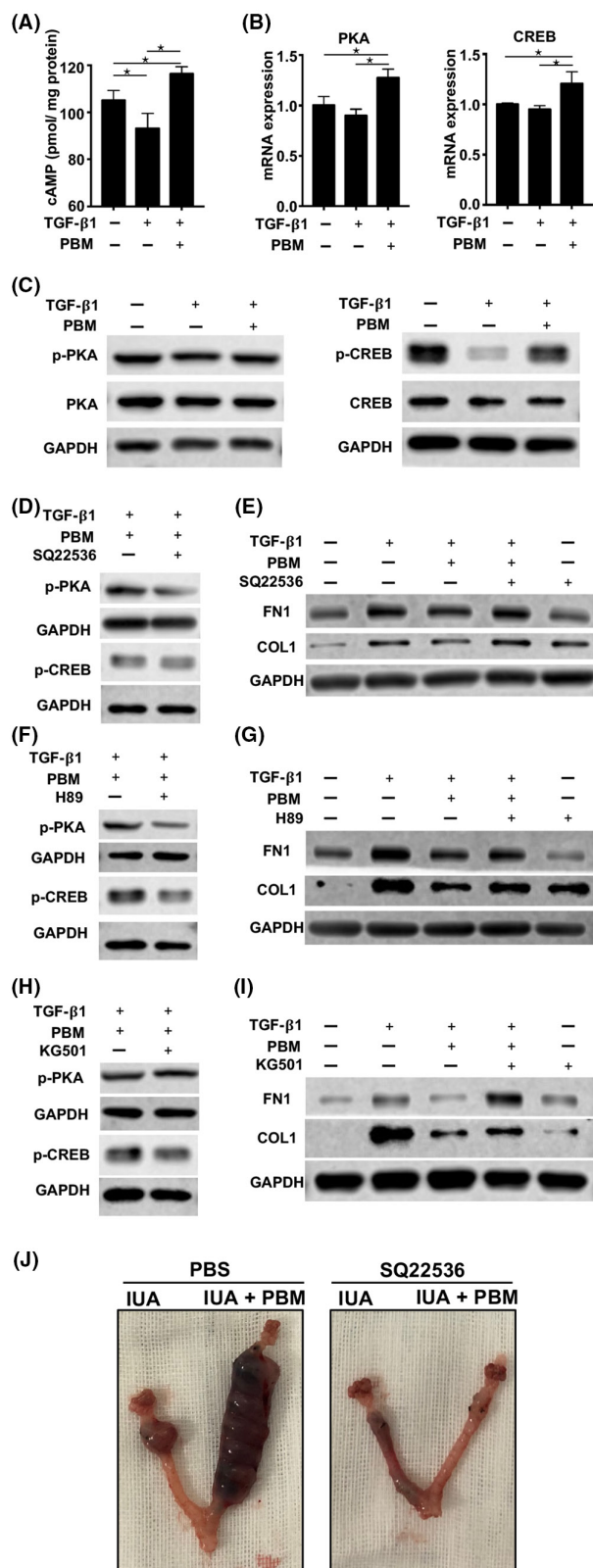
This study investigated the therapeutic effect of PBM on IUA. Our data demonstrated that PBM at 632 nm significantly alleviated the endometrial structural aberration and fertility dysfunction, and attenuated endometrial

fibrosis through the activation of cAMP/PKA/CREB signaling pathway in IUA.

Basal endometrial layer damage caused by intrauterine surgery, such as hysteroscopic surgery or induced abortion, is the major cause of IUA. It may lead to abnormal menstrual bleeding, intrauterine inflammation, scar tissue formation, and difficulty in preserving fertility.<sup>1</sup> Consequently, the primary goal in treating IUA is to prevent scarring of uterus and rescue the function of endometrium. Hysteroscopic adhesiolysis combined with adjuvant therapies, such as IUD placement, balloon placement, and estrogen application, remains the standard IUA treatment.<sup>22,23</sup> Although the resection of adhesions achieves immediate morphologic recovery of the uterine cavity, the recurrence rate for adhesions is as high as 20%–63%, while the pregnancy rate after hysteroscopic management is only 52%.<sup>3,24</sup> Adjuvant therapies also pose health risks due to systemic hormones or implant-related concerns. Therefore, there is an urgent need to develop a promising strategy for IUA patients to safely and effectively recover both the morphology and function of their injured uteri.

Photobiomodulation has been discovered over the last five decades and has shown the potential in healing wound, reducing inflammation, and relieving pain by increasing the expression of anti-inflammatory cytokines, downregulating pro-inflammatory cytokines expression, and reducing oxidative stress.<sup>5–7,25–28</sup> As promoting wound healing and reducing inflammation are key to treating IUA, we speculate that PBM may also alleviate IUA through these aspects, which requires further investigations. Fibrosis represents the terminal state of dysregulated repairing responses to injury, infection, inflammation, and immune responses of tissues.<sup>29</sup> The treatments for fibrosis normally involve reducing fibroblast proliferation, suppressing the secretion of pro-fibrotic cytokines, and reducing collagen synthesis and deposition.<sup>30</sup> According to previous reports, red and infrared PBM could reduce tissue fibrosis in the lungs, kidneys, skin, pulp, muscles, and tendons.<sup>9,30–34</sup> Besides, PBM has been reported to alleviate radiation fibrosis syndrome caused by cancer radiation therapy.<sup>35</sup> Consistent with these reports, our study confirmed that PBM improved endometrial fibrosis in IUA rats in vivo and TGF- $\beta$ 1-induced ESCs fibrosis in vitro. In addition, re-epithelialization of the endometrium is essential for its recovery following pathological injury and scar-free repair after a physiological menstrual breakdown in humans.<sup>36</sup> Our findings herein indicated that PBM increased the expression of CK18, an EECs-specific marker, suggesting improved endometrium integrity. PBM intervention induced a much better outcome in the IUA uterus, indicating the potential of PBM in the morphological recovery of injured uteri.





Fertility restoration is a major concern in IUA treatment.<sup>1</sup> The application of PBM for infertility has attracted attention since the early 2000s. A study in 2012 recruited 775 Japanese women with severe infertility after at least 4 years of failure with assisted reproductive technology (ART).<sup>37</sup> After an average of 15 treatments of PBM

**FIGURE 5** Photobiomodulation (PBM) attenuates fibrosis through the cAMP signaling pathway. (A–C) Endometrial stromal cells (ESCs) were treated with 5 ng/mL TGF- $\beta$ 1 with/without PBM. The cAMP content (A) was measured via ELISA and PKA and CREB expressions were evaluated by qPCR (B) and WB (C). \* $p < 0.05$ . (D–I) ESCs were treated with/without different cAMP signaling inhibitors and the protein expressions of p-PKA, p-CREB, FN1, and COL1 were evaluated. (J) Pregnant outcomes of intrauterine adhesion (IUA) rats at gestational day 15–18. Pretreatment with SQ22536 eliminated the effect of PBM on the functional restoration of the injured uterus.

at 830 nm, with or without ART, 22.2% of these patients became pregnant, and 11.6% achieved successful live delivery. Faham<sup>10</sup> employed PBM to explore its impacts on EECs and the underlying mechanisms and proved that PBM at 635 nm increased EECs proliferation and upregulated the expression of receptivity genes (ITGAV, ITGB3, MUC1, and LIF). The effects of PBM on EECs were also confirmed by Gebril in 2021.<sup>11</sup> The pregnancy outcome is the gold standard for verifying endometrial function recovery.<sup>36</sup> In our study, we observed that the pregnancy rate in IUA rats was remarkably higher after PBM. Using Trypan Blue staining and IHC for Ki67, early implantation sites and the proliferation of the endometrium on E 4.5 were analyzed, which reflected the endometrial receptivity. Our data reflected a higher embryonic implantation rate of the IUA + PBM group relative to the IUA group, which can be attributed to the restored endometrial function, suggesting the PBM-induced amelioration of receptivity in the injured uterus. Taken together, we believe that PBM can be used to treat IUA and facilitate the recovery of uterine reproductive function.

The mechanism underlying endometrial reconstruction remains unclear. By targeting chromophores with different wavelengths and parameters of laser, PBM can induce photochemical and photobiological effects in treating various diseases without causing thermal injury.<sup>4,38</sup> cAMP is an important secondary messenger produced from ATP by adenylyl cyclase (AC).<sup>39</sup> cAMP has been shown to exert a crucial function in regulating cellular processes and signaling pathways. In particular, the cAMP/PKA/CREB pathway has been implicated with several organ fibrotic diseases, and cAMP-elevating agents have been used to treat fibrosis.<sup>39–42</sup> Upon absorption by cytochrome C oxidase (CCO) located on the mitochondrial respiration chain complex IV, PBM stimulates the photodissociation of the inhibitory nitric oxide (NO) from CCO, generating a proton electrochemical gradient, which results in elevated levels of intracellular ATP and cAMP.<sup>4,20</sup> In this study, ELISA and western blotting showed that PBM increased levels of intracellular cAMP and phosphorylated PKA and CREB. Moreover, treatment with inhibitors targeting the cAMP/PKA/CREB

pathway decreased the anti-fibrotic effects of PBM in vitro and the pro-reproductive effects in vivo. Notably, although the off-target effects of SQ22536 when applied in vivo were not founded in our study as well as several other researches,<sup>43-45</sup> the exact tissue distribution and pharmacokinetics of SQ22536 have not been elucidated and need to be studied in the future.<sup>46</sup> Our study is the first to prove that PBM alleviates IUA via triggering the cAMP/PKA/CREB signaling pathway; however, this should be further investigated in detail in the future.

In conclusion, our study clarified the effectiveness of PBM at 632 nm for restoring endometrial morphology, receptivity, and fertility in IUA. Moreover, cAMP/PKA/CREB signaling pathway activation is critical for the effect of PBM in reducing endometrial fibrosis and restoring reproductive function both in vitro and in vivo. To our knowledge, our work is the first to demonstrate the pivotal role of PBM in repairing the injured endometrium and improving the pregnancy rate in IUA rats. Therefore, PBM may be a potential strategy for treating IUA and possibly other infertility conditions. PBM is a safe, non-invasive treatment modality that can be clinically applied intrauterine through hysteroscopy in the future for convenience and safety.

## ACKNOWLEDGMENTS

This work was financially supported by the National Key Research Program of China (Grant No. 2018YFC1004803 and 2020YFC1512704) and Shanghai Clinical Research Center of Plastic and Reconstructive Surgery supported by Science and Technology Commission of Shanghai Municipality (Grant No. 22MC1940300). We would like to thank Chao Fang and Youzhen Shi for kindly providing technical support.

## ORCID

Min Yao  <https://orcid.org/0000-0002-6946-8766>

## REFERENCES

- Yu D, Wong YM, Cheong Y, Xia E, Li TC. Asherman syndrome – one century later. *Fertil Steril*. 2008;89:759-779.
- Khan Z, Goldberg JM. Hysteroscopic management of Asherman's syndrome. *J Minim Invasive Gynecol*. 2018;25:218-228.
- Yang JH, Chen CD, Chen SU, Yang YS, Chen MJ. The influence of the location and extent of intrauterine adhesions on recurrence after hysteroscopic adhesiolysis. *BJOG*. 2016;123:618-623.
- Dompe C, Moncrieff L, Matys J, et al. Photobiomodulation—underlying mechanism and clinical applications. *J Clin Med*. 2020;9:1724.
- Percival SL, Francolini I, Donelli G. Low-level laser therapy as an antimicrobial and antibiofilm technology and its relevance to wound healing. *Future Microbiol*. 2015;10:255-272.
- John SS, Mohanty S, Chaudhary Z, Sharma P, Kumari S, Verma A. Comparative evaluation of low level laser therapy and cryotherapy in pain control and wound healing following orthodontic tooth extraction: a double blind study. *J Craniomaxillofac Surg*. 2020;48:251-260.
- Barretto SR, de Melo GC, dos Santos JC, et al. Evaluation of anti-nociceptive and anti-inflammatory activity of low-level laser therapy on temporomandibular joint inflammation in rodents. *J Photochem Photobiol B*. 2013;129:135-142.
- Sassoli C, Chellini F, Squecco R, et al. Low intensity 635 nm diode laser irradiation inhibits fibroblast-myofibroblast transition reducing TRPC1 channel expression/activity: new perspectives for tissue fibrosis treatment. *Lasers Surg Med*. 2016;48:318-332.
- Terayama AM, Benetti F, de Araújo Lopes JM, et al. Influence of low-level laser therapy on inflammation, collagen fiber maturation, and tertiary dentin deposition in the pulp of bleached teeth. *Clin Oral Investig*. 2020;24:3911-3921.
- El Faham DA, Elnoury MAH, Morsy MI, El Shaer MA, Nour Eldin GM, Azmy OM. Has the time come to include low-level laser photobiomodulation as an adjuvant therapy in the treatment of impaired endometrial receptivity? *Lasers Med Sci*. 2018;33:1105-1114.
- Gebriil M, Aboelmaaty A, Al Balah O, Taha T, Abbassy A, Elnoury MAH. Bio-modulated mice epithelial endometrial organoids by low-level laser therapy serves as an invitro model for endometrial regeneration. *Reprod Biol*. 2021;21:100564.
- Zhang SS, Xia WT, Xu J, et al. Three-dimensional structure micelles of heparin-ploxamer improve the therapeutic effect of 17 $\beta$ -estradiol on endometrial regeneration for intrauterine adhesions in a rat model. *Int J Nanomedicine*. 2017;12:5643-5657.
- Marquardt RM, Kim TH, Yoo JY, et al. Endometrial epithelial ARID1A is critical for uterine gland function in early pregnancy establishment. *FASEB J*. 2021;35:e21209.
- Ceccarelli S, D'Amici S, Vescarelli E, et al. Topical KGF treatment as a therapeutic strategy for vaginal atrophy in a model of ovariectomized mice. *J Cell Mol Med*. 2014;18:1895-1907.
- Zhang S, Li P, Yuan Z, Tan J. Platelet-rich plasma improves therapeutic effects of menstrual blood-derived stromal cells in rat model of intrauterine adhesion. *Stem Cell Res Ther*. 2019;10:61.
- Lee Y, Kim H, Hong N, Ahn JC, Kang HW. Combined treatment of low-level laser therapy and phloroglucinol for inhibition of fibrosis. *Lasers Surg Med*. 2020;52:276-285.
- Lessey BA, Young SL. What exactly is endometrial receptivity? *Fertil Steril*. 2019;111:611-617.
- Cai H, Li H, He Y. Interceed and estrogen reduce uterine adhesions and fibrosis and improve endometrial receptivity in a rabbit model of intrauterine adhesions. *Reprod Sci*. 2016;23:1208-1216.
- Monsivais D, Clementi C, Peng J, et al. BMP7 induces uterine receptivity and blastocyst attachment. *Endocrinology*. 2017;158:979-992.
- Karu T. Primary and secondary mechanisms of action of visible to near-IR radiation on cells. *J Photochem Photobiol B*. 1999;49:1-17.
- Hu WP, Wang JJ, Yu CL, Lan CC, Chen GS, Yu HS. Helium-neon laser irradiation stimulates cell proliferation through photostimulatory effects in mitochondria. *J Invest Dermatol*. 2007;127:2048-2057.
- Ma J, Zhan H, Li W, et al. Recent trends in therapeutic strategies for repairing endometrial tissue in intrauterine adhesion. *Biomater Res*. 2021;25:40.

23. Kou L, Jiang X, Xiao S, Zhao YZ, Yao Q, Chen R. Therapeutic options and drug delivery strategies for the prevention of intrauterine adhesions. *J Control Release*. 2020;318:25-37.
24. Capmas P, Mihalache A, Duminil L, Hor LS, Pourcelot AG, Fernandez H. Intrauterine adhesions: what is the pregnancy rate after hysteroscopic management? *J Gynecol Obstet Hum Reprod*. 2020;49:101797.
25. Mester E, Szende B, Gärtner P. The effect of laser beams on the growth of hair in mice. *Radiobiol Radiother*. 1968;9:621-626.
26. Taradaj J, Shay B, Dymarek R, et al. Effect of laser therapy on expression of angio- and fibrogenic factors, and cytokine concentrations during the healing process of human pressure ulcers. *Int J Med Sci*. 2018;15:1105-1112.
27. Ahmed OM, Mohamed T, Moustafa H, Hamdy H, Ahmed RR, Aboud E. Quercetin and low level laser therapy promote wound healing process in diabetic rats via structural reorganization and modulatory effects on inflammation and oxidative stress. *Biomed Pharmacother*. 2018;101:58-73.
28. Yamaura M, Yao M, Yaroslavsky I, Cohen R, Smotrich M, Kochevar IE. Low level light effects on inflammatory cytokine production by rheumatoid arthritis synoviocytes. *Lasers Surg Med*. 2009;41:282-290.
29. Henderson NC, Rieder F, Wynn TA. Fibrosis: from mechanisms to medicines. *Nature*. 2020;587:555-566.
30. Mamalis A, Siegel D, Jagdeo J. Visible red light emitting diode photobiomodulation for skin fibrosis: key molecular pathways. *Curr Dermatol Rep*. 2016;5:121-128.
31. de Brito AA, da Silveira EC, Rigonato-Oliveira NC, et al. Low-level laser therapy attenuates lung inflammation and airway remodeling in a murine model of idiopathic pulmonary fibrosis: relevance to cytokines secretion from lung structural cells. *J Photochem Photobiol B*. 2020;203:111731.
32. Oliveira FA, Moraes AC, Paiva AP, et al. Low-level laser therapy decreases renal interstitial fibrosis. *Photomed Laser Surg*. 2012;30:705-713.
33. Fillipin LI, Mauriz JL, Vedovelli K, et al. Low-level laser therapy (LLLT) prevents oxidative stress and reduces fibrosis in rat traumatized Achilles tendon. *Lasers Surg Med*. 2005;37:293-300.
34. Alves AN, Fernandes KP, Melo CA, et al. Modulating effect of low level-laser therapy on fibrosis in the repair process of the tibialis anterior muscle in rats. *Lasers Med Sci*. 2014;29:813-821.
35. Tam M, Arany PR, Robijns J, Vasconcelos R, Corby P, Hu K. Photobiomodulation therapy to mitigate radiation fibrosis syndrome. *Photobiomodul Photomed Laser Surg*. 2020;38:355-363.
36. Xin L, Lin X, Pan Y, et al. A collagen scaffold loaded with human umbilical cord-derived mesenchymal stem cells facilitates endometrial regeneration and restores fertility. *Acta Biomater*. 2019;92:160-171.
37. Ohshiro T. Personal overview of the application of LLLT in severely infertile Japanese females. *Laser Ther*. 2012;21:97-103.
38. Karu TI. Mitochondrial signaling in mammalian cells activated by red and near-IR radiation. *Photochem Photobiol*. 2008;84:1091-1099.
39. Métrich M, Berthouze M, Morel E, Crozatier B, Gomez AM, Lezoualc'h F. Role of the cAMP-binding protein Epac in cardiovascular physiology and pathophysiology. *Pflugers Arch*. 2010;459:535-546.
40. Delaunay M, Osman H, Kaiser S, Diviani D. The role of cyclic AMP signaling in cardiac fibrosis. *Cell*. 2019;9:69.
41. Insel PA, Murray F, Yokoyama U, et al. cAMP and Epac in the regulation of tissue fibrosis. *Br J Pharmacol*. 2012;166:447-456.
42. Wójcik-Pszczola K, Chłoń-Rzepa G, Jankowska A, et al. A novel, Pan-PDE inhibitor exerts anti-fibrotic effects in human lung fibroblasts via inhibition of TGF- $\beta$  signaling and activation of cAMP/PKA signaling. *Int J Mol Sci*. 2020;21:4008.
43. Guo M, Cui C, Song X, et al. Deletion of FGF9 in GABAergic neurons causes epilepsy. *Cell Death Dis*. 2021;12:196.
44. Liou JT, Liu FC, Hsin ST, Yang CY, Lui PW. Inhibition of the cyclic adenosine monophosphate pathway attenuates neuropathic pain and reduces phosphorylation of cyclic adenosine monophosphate response element-binding in the spinal cord after partial sciatic nerve ligation in rats. *Anesth Analg*. 2007;105:1830-1837, table of contents.
45. Marks GA, Birabil CG. Infusion of adenylyl cyclase inhibitor SQ22,536 into the medial pontine reticular formation of rats enhances rapid eye movement sleep. *Neuroscience*. 2000;98:311-315.
46. Seifert R, Lushington GH, Mou TC, Gille A, Sprang SR. Inhibitors of membranous adenylyl cyclases. *Trends Pharmacol Sci*. 2012;33:64-78.

## SUPPORTING INFORMATION

Additional supporting information can be found online in the Supporting Information section at the end of this article.

**How to cite this article:** Zheng H, Wang C, Wu S, Pei Q, Yao M. Photobiomodulation therapy at 632 nm wavelength ameliorates intrauterine adhesion via activation of cAMP/PKA/CREB pathway. *Photochem Photobiol*. 2024;100:214-224. doi:[10.1111/php.13813](https://doi.org/10.1111/php.13813)